Pyramid-Based Multi-structure Local Binary Pattern for Texture Classification

Yonggang He, Nong Sang, and Changxin Gao

Institute for Pattern Recognition and Artificial Intelligence
Huazhong University of Science and Technology
Wuhan, Hubei 430074, China

Abstract. Recently, the local binary pattern (LBP) has been widely used in texture classification. The conventional LBP methods only describe micro structures of texture images, such as edges, corners, spots and so on, although many of them show a good performance on texture classification. This situation still could not be changed, even though the multiresolution analysis technique is used in methods of local binary pattern. In this paper, we investigate the drawback of conventional LBP operators in describing some textures that has the same small structures but differential large structures. And a multi-structure local binary pattern operator is achieved by executing the LBP method on different layers of image pyramid. The proposed method is simple yet efficient to extract not only the micro structures but also the macro structures of texture images. We demonstrate the performance of our method on the task of rotation invariant texture classification. The experimental results on Outex database show advantages of the proposed method.

1 Introduction

Texture classification has been extensively investigated during the last several decades. Some methods for texture classification focus on the statistical analysis of texture images. The representative methods include the co-occurrence matrix method [2] and filtering based approaches [5, 11, 15]. Varma and Zisserman [16] present a good statistical algorithm, MR8, which uses 38 filters to build a rotation invariant texton library from a training set for classifying an unknown texture image. Recently, a simple but more powerful operator the local binary pattern (LBP) [13] that is based on the signs of differences of neighboring pixels is used for image description. And it has been successfully applied to texture analysis [10]. For texture classification, Ojala et al. [12] show a good performance of LBP for texture classification by comparing with other methods. And Mäenpää et al. [8] introduce a uniform pattern to robust texture description by selecting subsets of patterns encoded in LBP forms. With this technique, they propose a rotation invariant uniform pattern (LBP^{riu2}) [14] to describe the texture image. By utilising the temporal domain information, Zhao and Pietikäinen [17] extend the LBP to the VLBP for dynamic texture classification. Ahonen et al. [1] use the local binary pattern histogram Fourier features (LBP-HF) to describe rotation texture. Guo et al. [3] take the local variance as a weight of local binary

R. Kimmel, R. Klette, and A. Sugimoto (Eds.): ACCV 2010, Part III, LNCS 6494, pp. 133–144, 2011.

pattern to adjust the contribution of the LBP code in histogram calculation and propose the LBPV operator for rotation invariant texture classification. Liao et al. [6] use the 80% dominant local binary pattern (DLBP) to classify the texture. And combining with Gabor features, it attains a high classification rate. The LBP-HF, LBPV and DLBP are both state-of-the-art algorithms and yield good results in the task of rotation invariant texture classification.

Although these operators perform well, most of them base on the same idea of LBP which only extracts isotropic micro structures of images. These micro structures are not enough to describe the texture information. The problem still can't be solved by the multiresolution LBP method [14] that just combines the limited neighbor sample points and radii. At the same time, the stability of LBP value deteriorates rapidly with the increasing of neighbor radius, because the sampling points have less correlation with the centre pixel with the present of larger radius. Multi-scale binary patterns (LBPF) [9] employs exponentially growing circular neighborhoods with Gaussian low-pass filtering to extract binary patterns for texture analysis. The LBPF also shows isotropic micro structures of images but a little bigger than the structures extracted by basic LBP methods. Our work considered the structures extracted by basic LBP. We carried out the rotation invariant uniform pattern LBP in an image pyramid to extract both micro and macro structures of texture images. The pyramid technique had been used in texture field by Heeger and Bergen [4] many years ago, but they focused on texture synthesis. In our work, four anisotropic filter templates ensured the collection of anisotropic structures in the image pyramid. Later, weights of different structural histograms were set to enhance the performance of proposed method. The results of experiment on Outex database show the superiority of our method.

The rest of this paper is organized as follows. Section 2 gives a brief overview of the basic LBP method and discusses the structures extracted by the conventional LBP. Section 3 devotes to the details of the proposed method. Section 4 presents the implementation of our experiments. Section 5 concludes his paper.

2 Local Binary Pattern

In this section, we review the LBP methods and points out the structures of texture images that are neglected by the conventional LBP. This is necessary for understanding the advantage of our method.

2.1 The LBP Methods

The local binary pattern (LBP) [14] is an illumination invariant texture operator which characterizes the local structure of the texture image. The basic LBP considers a small circularly symmetric neighborhood that has P equally spaced pixels on a circle of radius R. The LBP value of the center pixel is computed by thresholding the gray value of P sampling point with their center value, and summing the thresholded values weighted by powers of two. Thus, the LBP label for the center pixel (x,y) is obtained by

$$LBP_{P,R}(x,y) = \sum_{p=0}^{P-1} s(g_p - g_c)2^p \tag{1}$$

$$s(x) = \begin{cases} 1, & x \geq 1 \\ 0, & x < 0 \end{cases} \tag{2}$$

where g_c is the gray value of the center pixel, g_p (p=0,...,*P-1*) correspond to the gray values of P sampling points. If the coordinates of g_c are (0,0), then the coordinates of g_p are given by $(-Rsin(2\pi p/P), Rcos(2\pi p/P))$. The gray values of neighbors which do not fall exactly in the center of grids are estimated by interpolation.

The rotation invariant version of LBP is achieved with the uniform measure. Mäenpää et al. [8] first defined the nonuniformity measure U ('pattern') as the number of transitions (0/1 or 1/0 changes) in the circular bitwise presentation of the LBP code. Later, Ojala et al. [14] designated patterns that have U value of at most 2 as 'uniform' and propose a rotation invariant uniform pattern operator $LBP^{riu2}_{P,R}$ for texture description:

$$LBP^{riu2}_{P,R} = \begin{cases} \sum_{p=0}^{P-1} s(g_p - g_c), & \text{if } U(LBP_{P,R}) \leq 2 \\ P+1, & otherwise \end{cases} \tag{3}$$

where

$$U(LBP_{P,R}) = \left|s(g_{P-1} - g_c) - s(g_0 - g_c)\right| + \sum_{p=1}^{P-1} \left|s(g_p - g_c) - s(g_{p-1} - g_c)\right| \tag{4}$$

According to the definition of 'uniform', there are P+1 'uniform' binary patterns in a circularly symmetric neighbor set of P pixels. Equ. (3) assigns a unique label to each of them, corresponding to the number of '1' bits in the pattern (0,1,...,P), while the 'non-uniform' patterns are grouped under the 'miscellaneous' label (P+1). Thus, the $LBP^{riu2}_{P,R}$ has P+2 distinct output values.

2.2 Structures Extracted by Conventional LBP

The uniform LBP, as a classical version of LBP, has achieved a good performance in texture analysis. Therefore, it is necessary to select the uniform LBP method to analysis the structures that are extracted by LBP. According to the definition of uniform, there are 58 different uniform patterns in (8,R) neighborhood. The pattern '0' means the gray values of P neighbor points smaller than the central pixel's, and corresponds to a plot structure. Patterns that have equal numbers of continuous '0' and '1' correspond to an edge structure. The pattern '255' correlates with two structures. If the gray values of P neighbor points greater than the central pixel's, the pattern expresses a plot structure. And the flat structure is described when the P neighbor points and their central pixel have the same

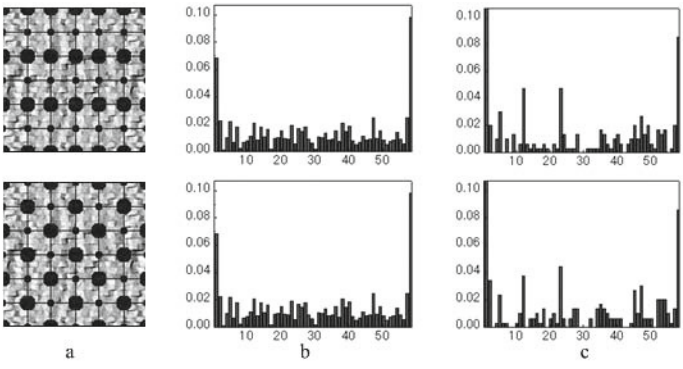

Fig. 1. 1st column: Two texture images have same micro structures. 2nd column: Uniform LBP (P=8, R=1) histograms of left textures. 3nd column: Uniform LBP (P=8, R=1) histograms of the second level of pyramid of left textures. All the histograms are normalized. The Euclidian distances of histograms in subimages (b) and (c) are 0.0029 and 0.0454, respectively.

gray value. The remained uniform patterns are 'L' type corners of the image. These structures are the micro structures of images because the conventional LBP methods only consider a small neighborhood. The non-uniform patterns also correspond to small structures ('Y' corner, 'X' corner, short line and so on).

The performance of conventional LBP is limited, because these methods only consider micro structures of images. The weakness is clear when different texture images have same micro structures. We give an extreme example in Fig. 1. In first column, there are two texture images which have same micro structures but different macro structures. The second column presents uniform LBP (P=8, R=1) histograms of the textures in first column. It's clearly that the uniform LBP worked on orignal images have no contribution to classify the two textures because they have similar LBP feature histograms. The third column gives uniform LBP (P=8, R=1) histograms of the second level of pyramid of texture images in first column. Some differences of the two histograms can be seen in the third colum. The details of image pyramid will be described in next section.

3 Multi-structure Local Binary Pattern

In image field, the isotropic means doing the same operation in every direction, while the anisotropic is just opposite. Studying from the section 2, we can easily find that the basic LBP only considers the isotropic micro structures of images, because it samples with equal space in a small circularly symmetric neighborhood. In this section, we execute the rotation invariant LBP on an image pyramid to extract three different kinds of structures: (1) isotropic micro structures; (2) isotropic macro structures; (3) anisotropic macro structures.

3.1 Image Pyramid

An image pyramid can be created from the original image. We use the sign $I_{l,t}$ to indicate sub-images of an image pyramid. The subscript l stands for the level of the image pyramid and t indicates what template is used to create the sub-image $I_{l,t}$. There are five templates in total. The first template is a 2-dimension Gaussian function $G(x, y, \sigma)$, which is used to smooth image. Referred to SIFT [7], we select the variance σ=1.5.

$$G(x, y, \sigma) = \frac{1}{2\pi\sigma^2} e^{-(x^2+y^2)/2\sigma^2} \tag{5}$$

Other four anisotropic filters $T_1 \sim T_4$ are used to create anisotropic sub-images of the pyramid. Fig. 2 shows the structures of templates $T_1 \sim T_4$. The templates $T_2 \sim T_4$ are created by rotating the template T_1 clockwise in three different angles (45°, 90° and 135 °).

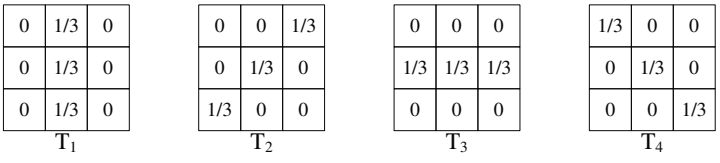

Fig. 2. Four templates ($T_1 \sim T_4$) for drawing anisotropic macro structures

The original image is $I_{0,0}$. The sub-image $I_{l,t}$ (l>0) are created from the image $I_{l-1,0}$ by the following formula:

$$I_{l-1,t} = \begin{cases} (I_{l,0} * G) \downarrow 2, & t = 0 \\ (I_{l,0} * T_t) \downarrow 2, & t = 1, \cdots, 4 \end{cases} \tag{6}$$

where * is the convolution operation, $\downarrow 2$ means downing sample by 2. Here, an approximation is used for extracting anisotropic sub-image by $\downarrow 2$ operation. This approximation is able to reduce the calculations and has little influence when an operation is implemented in small neighborhood. Fig. 3 gives a three-level pyramid for extracting different structures.

3.2 Rotation Invariant Multi-structure Local Binary Pattern

The multi-structure local binary pattern (*Ms-LBP*) can be achieved by running the basic LBP on the image pyramid. The isotropic and anisotropic macro structures are obtained by LBP methods in the sub-images $I_{l,0}$ (l>0) and $I_{l,t}$(l >0,t=1,2,3,4), respectively. The isotropic micro structures are obtained by LBP methods in original image. Similarly, the rotation invariant multi-structure binary pattern can be achieved by carrying out the rotation invariant uniform pattern operator $LBP^{riu2}_{P,R}$ on different pyramid levels. Thus, the sign of our method

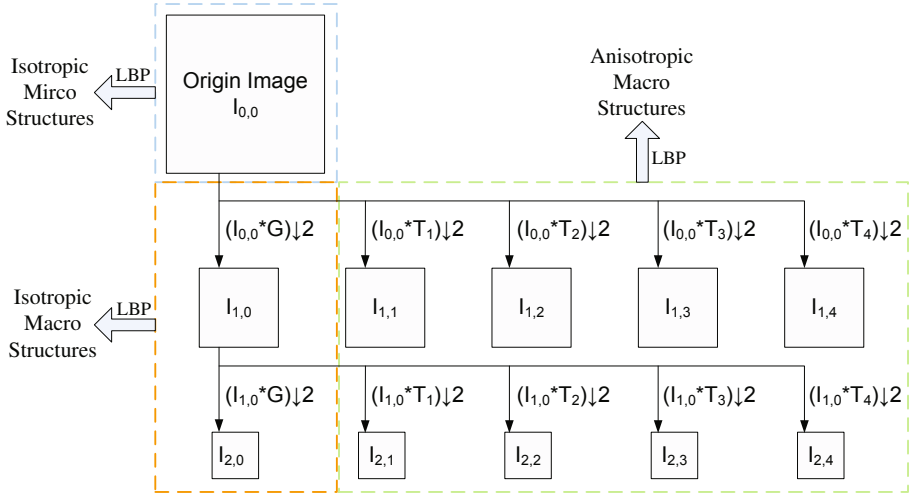

Fig. 3. Extraction of multi-structures in a three-level pyramid

is rewritten as $Ms\text{-}LBP^{riu2}_{P,R}$, where 'P', 'R' and 'riu2' have the same meaning with the operator $LBP^{riu2}_{P,R}$. The final histogram of $Ms\text{-}LBP^{riu2}_{P,R}$ is grouped with $LBP^{riu2}_{P,R}$ histograms of every single sub-images of pyramid:

$$H_{l,t}(k) = \sum_{i=1}^{N}\sum_{j=1}^{M} f(LBP^{riu2}_{l,t,P,R}(i,j),k), k \in [0,K] \tag{7}$$

$$f(x,y) = \begin{cases} 1, & x = y \\ 0, & otherwise \end{cases} \tag{8}$$

where $LBP^{riu2}_{l,t,P,R}(i,j)$ is the $LBP^{riu2}_{P,R}$ value of pixel $I_{l,t}(i,j)$; K is the maximal pattern, $H_{l,t}$ is the $LBP^{riu2}_{P,R}$ histogram of the sub-image $I_{l,t}$; M and N are the sizes of the sub-image of the pyramid.

3.3 Similarity Metric

The similarity of sample and model histograms can be evaluated by a test of goodness-of-fit, which is measured with a nonparametric statistical test. The nonparametric test can avoid making any assumptions about the feature distributions. The log-like distance that is employed by many literatures [9, 14, 17] is a goodness-of-fit statistics and useful for measuring the similar between histograms. The log-like distance between a model M and a sample S is computed as follow:

$$D(S,M) = \sum_{b=1}^{B} S_b \log(M_b) \tag{9}$$

where B is the number of bins and S_b and M_b are, respectively, the values of the sample and model images at the bth bin.

The final similarity distance contains three parts because of the existing of three different kinds of structures. Considering the rotation variance of texture images, we take four anisotropic sub-images $I_{l,t}(l > 0, t = 1, \cdots, 4)$ in one level as a whole to compute the distance. And the procedure is iteratively run four times to find the minimal similarity as the distance of anisotropic macro structures. Comparing with the micro structures, the macro structures located in the pyramid top show little statistical because of the small sizes of sub-images in high levels. Intuitively, the distances of structures on higher level make fewer contributions to classifying samples than the distances of structures on lower level. Thus, the final similarity distance ($D_F(S, M)$) is computed by adding the three groups of distance with different weights in different levels:

$$D_F(S,M) = w_{0,0}D(S_{0,0}, M_{0,0}) + \sum_{l=1}^{L} w_{l,0}D(S_{l,0}, M_{l,0}) + \sum_{l=1}^{L} w_{l,1}D_{min}(S_l^{an}, M_l^{an})$$

$$\begin{cases} D_{min}(S_l^{an}, M_l^{an}) = \dfrac{1}{4}\displaystyle\sum_{t=1}^{4} D(S_{l,mod(t+k-1,4)+1}, M_{l,t}) \\ k = \arg\min\limits_{j}(\displaystyle\sum_{l=1}^{L}\sum_{t=1}^{4} D(S_{l,mod(t+j-1,4)+1}, M_{l,t}), j = 0, 1, 2, 3) \end{cases} \tag{10}$$

where $S_{l,t}$ and $M_{l,t}$ stand for sub-images of pyramid of sample S and model M, respectively; w are the distant weights and L is the maximum level of the image pyramid.

The classification rate is a good candidate as the distant weight. There are two parts in every level of the image pyramid except level zero. One part is used for obtaining isotropic macro structures and the other part is used for collecting anisotropic macro structures. But the *0*th level of the image-pyramid is an exception, because there is only a sub-image $I_{0,0}$ that is used to extracted isotropic micro structures. We use one part of the pyramid at a time to achieve the task of rotation invariant texture classification. Different parts get different classification rates which correspond to different weights. The result of a log-like distance between two histograms is always a nonpositive value. Therefore, the normalized wrong classification rates are selected as the distance weights.

4 Experimental Results

We demonstrate the performance of our operators on the public texture database, Outex, which is used to study rotation invariant texture classification by many literatures [1, 3, 14]. We used this database because their texture images are acquired under more varied conditions (viewing angle, orientation and source of illumination) than the widely used Brodatz database. There are 24 classes of textures in Outex database. And these textures are collected under three illuminations and

at nine angles. Our experiments were performed on two test suites of Outex: Outex_TC_00010 (TC10) and Outex_TC_00012 (TC12). TC10 is used for studying rotation invariant texture classification and TC12 is used for researching illuminant and rotation invariant texture classification. The two test suites contain the same 24 classes of textures as shown in Fig. 4. Each texture class is collected under three different illuminants ('inca', 't184' and 'horizon') and nine different angles of rotation (0°, 5°, 10°, 15°, 30°, 45°, 60°, 75° and 90°).

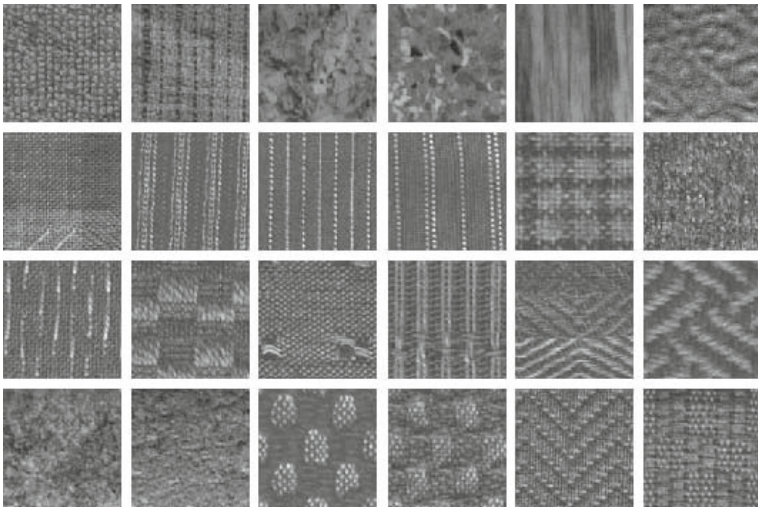

Fig. 4. 128×128 samples of the 24 textures from Outex database

There are 20 non-overlapping 128×128 texture samples for each class under each setting. The experimental setups are as follows:

1. For TC10, classifiers were trained with the reference textures of illuminant 'inca' (20 samples of angle 0° in each texture class), while the 160 (8×20) samples of the other eight rotation angles in each texture class were used for testing the classifier. Hence, there were 480 (24×1×20) models and 3840 (24×8×20) testing samples in total.

2. For TC12, classifiers were trained with the reference textures (20 samples of illuminant 'inca' and angle 0° in each texture class) and tested with all samples captured under illuminant 'tl84' or 'horizon'. Hence, in both of the two illuminant experiments, there are 480 (24×20) models and 4320 (24×20×9) validation samples in total for each illuminant. In order to simplify the name of TC12 test suite, 'TC12t' is short for TC12 'tl84' test suite, and 'TC12h' is short for TC12 'horizon' test suite.

4.1 Calculation of Distance Weights

Both TC12 and TC10 have the same training set that contains 480 samples of illuminant 'inca' in total. There are 20 samples of angle 0° in each texture.

The distance weights were learned on the training set of TC12 and TC10, although the training samples have some differences with the testing samples in angles and illuminants. One sample of each texture was selected as a new training sample for the training classifier at a time, the rest of samples (19×24 samples) were used to test the classifier. We executed the process twenty times, and twenty classification results were given by dividing the samples sets twenty times. The final classification results were the average of the twenty results. In the experiments, the $LBP^{riu2}_{P,R}$ histograms of different parts of pyramid were used to calculate the classification rates. Table 1 presents the right classification rate of different parts of the pyramid in three different sample points P and radius R. The sign '–' in Table 1 presents that no anisotropic structures are extracted in level zero. Five levels are extracted on 128×128 image.

Table 1. Right classification rates (%) with different parts of image pyramid on the training sets of TC10 and TC12

	Isotropic Parts					Anisotropic Parts				
P,R	level0	level1	level2	level3	level4	level0	level1	level2	level3	level4
8,1	76.75	70.78	50.60	38.37	13.44	–	77.21	73.67	48.53	18.43
16,2	81.55	74.44	55.71	33.62	8.66	–	77.98	70.21	38.22	8.00
24,3	81.68	76.79	55.31	13.32	5.04	–	81.88	65.42	15.43	4.67

Results in Table 1 present that the classification rates deteriorate rapidly with the increase of levels, because the sizes of images in high levels are too small to supply enough statistics of structures. Four anisotropic templates cause more anisotropic structures to be extracted than isotropic structures, and give a good performance to the anisotropic parts of image pyramid. As can be seen from Table 1, the classification rates of anisotropic parts are usually higher than the results of isotropic parts in the same levels of image pyramid.

The distance weights were computed by normalizing the wrong classification rates which were obtained by subtracting the correct classification rates from one. Table 2 shows the value of distance weights with different (P, R).

Table 2. Distance weights of different structures

	Isotropic Parts					Anisotropic Parts				
P,R	level0	level1	level2	level3	level4	level0	level1	level2	level3	level4
8,1	0.05	0.07	0.11	0.14	0.20	–	0.05	0.06	0.12	0.19
16,2	0.04	0.06	0.10	0.15	0.20	–	0.05	0.07	0.14	0.20
24,3	0.04	0.05	0.09	0.17	0.19	–	0.04	0.07	0.17	0.19

4.2 Implementation of Multi-structure Local Binary Pattern

The performance of texture classification algorithms is characterized with the percentage of correctly classified samples. The best results of each test suite in experiment are marked in bold font. Five-layered pyramid were used in the experiment according to the size of testing images. Weights in Table 2 were combined with the distances of different parts of the image pyramid to calculate similarity between samples and models. We employed the 3-NN method as a classification principle that has been used by other literatures [9, 14]. The effects of proposed method were compared against six methods: LBP^{riu2}, LBP^{riu2}/VAR, LBP-HF, $LBPV^{u2}_{P,R}GM_{ES}$, $DLBP$ and $MR8$. The method LBP^{riu2} is a useful rotation invariant method. And combining with local variance (VAR), LBP^{riu2}/VAR obtains a good performance. LBP histogram Fourier features (LBP-HF), LBP variance with global matching ($LBPV^{u2}_{P,R}GM_{ES}$) and dominant local binary patterns ($DLBP$) are improved versions of basic LBP. For comparing, we gave the results of $DLBP$ under best parameters ($DLBP_{R=3} + NGF$) in Table 3. $MR8$ is a state-of-the-art statistical algorithm.

Table 3 shows the advantages of the proposed method. The high scores 99.30%, 98.26% and 97.08% are obtained by the operator $Ms\text{-}LBP^{riu2}_{16,2}$ on three different suits(TC10, TC12t and TC12h), respectively. The superiority of our method is obvious on the test suits TC12 which contains both illuminant and rotation variant of textures. Textures under different illuminant usually have different micro structures, but their macro structures are very similar. Thus, compared with other operators, our method works well on testing sets TC12. It could find that the $Ms\text{-}LBP^{riu2}_{P,R}$ method usually excel its counterparts under the same parameters (P,R) and in the same testing sets. This situation is particularly clear when the parameter (P,R) equals to (8,1) because macro structures are also extracted in $Ms\text{-}LBP^{riu2}_{8,1}$. The best results of our method are obtained with parameter (16, 2). And the performance degrades a little with parameter (24,3). The phenomenon is distinct in Table 1, especially the results on large levels of image pyramid. Because the sizes of sub-image in high level of image pyramid are very small, the total numbers of feature is very few. At the same time, the dimension of histogram increases with the number of sampling points P. It's known that a high-dimensional histogram with few features is not enough to describe the distribution of features in the statistical sense. And the operator $Ms\text{-}LBP^{riu2}_{24,3}$ belongs to this situation. As can be seen from the Table 3, the performance of $Ms\text{-}LBP^{riu2}_{P,R}$ degrades a little with large sample points P=24, because the high levels of image pyramid supply few feature with large number of bins of the histogram.

Although good results are obtained, our method needs more time to classify a texture than most LBP operators. We select the best parameter (P,R)=(16,2) and execute these operators on a computer with the Intel CPU 2.8GHz. Our method needs 0.466s to classify a texture, while $LBP^{riu2}_{P,R}$ only needs 0.012s. The classification time of our method is less than the MR8 operator (2.257s), because the MR8 needs to find 8 maximum responses after 38 filters convoluting with

Table 3. Correct Classification rate (%) for TC10 and TC12 using different methods

P,R	8,1			16,2			24,3		
	TC10	TC12t	TC12h	TC10	TC12t	TC12h	TC10	TC12t	TC12h
$LBP^{riu2}_{P,R}$	83.31	69.86	62.94	92.29	86.25	83.61	96.38	89.81	88.75
$LBP^{riu2}_{P,R}/VAR_{P,R}$	95.81	78.73	77.27	97.97	87.06	85.90	97.48	86.81	87.27
$LBP\text{-}HF_{P,R}$	83.26	76.20	78.45	93.93	88.15	86.46	97.97	91.50	87.66
$LBPV^{u2}_{P,R}GM_{ES}$	73.64	72.47	76.57	93.90	90.25	94.28	97.76	95.39	95.57
$MS\text{-}BP^{u2}_{P,R}$	97.87	94.98	91.76	**99.30**	**98.26**	**97.08**	98.26	96.46	94.72
$MR8$	92.5(TC10), 90.9(TC12t), 91.1(TC12h)								
$DLBP_{R=3}+NGF$	99.1(TC10), 93.2(TC12t), 90.4(TC12h)								

the image and compare very 8-dimension vector in an image with all the textons to build histograms.

5 Conclusions

The conventional LBP methods only focus on micro structures of images, although they have already been powerful in texture analysis. In this paper, we executed the rotation invariant uniform LBP on the image pyramid to extract three different structures (isotropic micro structures, isotropic macro structures and anisotropic macro structures). The experiment results on Outex database demonstrate the advantages of our method. The performance of proposed method is limited by the size of images, because small images are not enough to supply large macro structures. Fortunately, the texture images are different from other images, due to they are full of repeat patterns. So in the future, some texture synthesis methods could be used to create large size texture image. And more stable multi-structure local binary patterns could be achieved on the synthesized texture images.

Acknowledgement. This work was supported by the Chinese National 863 Grand No. 2009AA12Z109.

References

1. Ahonen, T., Matas, J., He, C., Pietikäinen, M.: Rotation invariant image description with local binary pattern histogram fourier features. In: Salberg, A.-B., Hardeberg, J.Y., Jenssen, R. (eds.) SCIA 2009. LNCS, vol. 5575, pp. 61–70. Springer, Heidelberg (2009)
2. Davis, L., Johns, S., Aggarwal, J.: Texture analysis using generalized co-occurrence matrices. IEEE Transactions on Pattern Analysis and Machine Intelligence 1, 251–259 (1979)

3. Guo, Z., Zhang, L., Zhang, D.: Rotation invariant texture classification using lbp variance (lbpv) with global matching. Pattern Recognition 43, 706–719 (2009)
4. Heeger, D.J., Bergen, J.R.: Pyramid-based texture analysis/synthesis. In: Proceedings of SIGGRAPH 1995, pp. 229–238 (1995)
5. Laine, A., Fan, J.: Texture classification by wavelet packet signatures. IEEE Transactions on Pattern Analysis and Machine Intelligence 15, 1186–1191 (1993)
6. Liao, S., Law, M., Chung, A.: Dominant local binary patterns for texture classification. IEEE Transactions on Image Processing 18, 1107–1118 (2009)
7. Lowe, D.: Distinctive image features from scale-invariant keypoints. International Journal of Computer Vision 60, 91–110 (2004)
8. Mäenpää, T., Ojala, T., Pietikäinen, M., Soriano, M.: Robust texture classification by subsets of local binary patterns. In: Proc. 15th International Conference on Pattern Recognition, Barcelona, Spain, pp. 947–950 (2000)
9. Mäenpää, T., Pietikäinen, M.: Multi-scale binary patterns for texture analysis. In: Bigun, J., Gustavsson, T. (eds.) SCIA 2003. LNCS, vol. 2749, pp. 885–892. Springer, Heidelberg (2003)
10. Mäenpää, T., Pietikäinen, M.: Texture analysis with local binary patterns. In: Handbook of Pattern Recognition and Computer Vision, 3rd edn., pp. 197–216. World Scientific, Singapore (2005)
11. Manjunath, B.S., Ma, W.Y.: Texture features for browsing and retrieval of image data. IEEE Transactions on Pattern Analysis and Machine Intelligence 18, 837–842 (1996)
12. Ojala, T., Pietikäinen, M., Harwood, D.: A comparative study of texture measures with classification based on featured distributions. Pattern Recognition 29, 51–59 (1996)
13. Ojala, T., Valkealahti, K., Oja, E., Pietikäinen, M.: Texture discrimination with multidimensional distributions of signed gray-level differences. Pattern Recognition 34, 727–739 (2001)
14. Ojala, T., Pietikäinen, M., Mäenpää, T.: Multiresolution gray-scale and rotation invariant texture classification with local binary patterns. IEEE Transactions on Pattern Analysis and Machine Intelligence 24, 971–987 (2002)
15. Randen, T., Husoy, J.: Filtering for texture classification: A comparative study. IEEE Transactions on Pattern Analysis and Machine Intelligence 21, 291–310 (1999)
16. Varma, M., Zisserman, A.: A statistical approach to texture classification from single images. International Journal of Computer Vision 62, 61–81 (2005)
17. Zhao, G., Pietikäinen, M.: Dynamic texture recognition using volume local binary patterns. In: Vidal, R., Heyden, A., Ma, Y. (eds.) WDV 2005/2006. LNCS, vol. 4358, pp. 165–177. Springer, Heidelberg (2007)